

Revealing the alkaline characteristic evolution of bauxite residue under biomass fermentation

by Wu, C., Li, C., Jiang, J., Hartley, W., Kong, X., Wu, Y. and Xue, S.

Copyright, publisher and additional information: .This is the authors' accepted manuscript. The published version is available via Springerlink.

Please refer to any applicable terms of use of the publisher.

DOI: <https://doi.org/10.1007/s11368-019-02482-5>



1 **Revealing the alkaline characteristic evolution of bauxite residue**
2 **under biomass fermentation**

3

4 **Chuan Wu¹ • Chuxuan Li¹ • Jun Jiang¹ • William Hartley² • Xiangfeng Kong¹ •**
5 **Yujun Wu¹ • Shengguo Xue**

6

7 ¹School of Metallurgy and Environment, Central South University, Changsha,
8 410083, China

9 ²Crop and Environment Sciences Department Harper Adams University Newport UK

10

11 ✉ Jun Jiang

12 junjiang@csu.edu.cn

13 ✉ Shengguo Xue

14 sgxue@csu.edu.cn

15

16 **Abstract**

17 Purpose: Biomass fermentation has been proposed as a simple and economical strategy
18 to alleviate the high alkalinity of bauxite residue. This study investigates the
19 neutralization of bauxite residue following the application of biomass as an alkali
20 modifier by natural fermentation.

21 Materials and methods: Fresh bauxite residue samples were collected from Pingguo
22 refinery (Aluminum Corporation of China). Samples were treated with straw mulching
23 (SC), straw mixing (SM), bagasse mulching (BC), and bagasse mixing (BM),
24 respectively. Treatments were analyzed for pH, EC, metal cations and soluble alkali
25 (OH^- , $\text{Al}(\text{OH})_4^-$ and CO_3^{2-}). The mineral phase and Na speciation were analyzed by X-
26 ray diffraction (XRD) and near-edge X-ray absorption fine structure (Na-XANES).

27 Results and discussion: Optimum application rate for either straw or bagasse was 20%
28 (w/w), reducing leachate pH from 10.26 to 8.56. During biomass transformation, the
29 alkaline mineral grossular was completely dissolved, whilst calcite and cancrinite were
30 dissolved to a lesser degree. No treatment changed the spatial distribution of Na^+ , but
31 the basic anions (OH^- , CO_3^{2-} and $\text{Al}(\text{OH})_4^-$) were significantly reduced.

32 Conclusions: Following treatment application, soluble alkali in the residues was
33 significantly reduced whilst the alkaline minerals were slightly dissolved. This was
34 determined as the main cause for the decrease in residue pH.

35

36 **Keywords** Bauxite residue • Biomass • Neutralization • Soluble alkali • Transformation

37

38 1 Introduction

39 Bauxite residue is a high-alkaline solid waste produced by digestion of bauxite
40 with caustic soda during the alumina production process (Xue et al. 2016a; Kong et al.
41 2017a). This process produces a high residue ratio, with a ton of alumina product
42 producing 1-2.0 tons of residue. This has led to the greatest emissions of any non-
43 ferrous metal smelting industry around the world (Xue et al. 2016b; Xu et al. 2010; Zhu
44 et al. 2017; Santini and Fey 2018). In 2018, the global stock of bauxite residue reached
45 4.6 billion tons and is still increasing with a rate of approximately 170 million tons
46 annually (Xue et al. 2019a; Zhu et al. 2016; Kong et al. 2018). Bauxite residue pH can
47 reach 10-13, with the corresponding leachate as high as 12-14 (Power et al. 2011; Li et
48 al. 2018; Santini and Fey 2015). The primary alkaline minerals associated with bauxite
49 residue include andradite ($\text{Ca}_3(\text{Fe}_{0.87}\text{Al}_{0.13})_2(\text{SiO}_4)_{1.65}(\text{OH})_{5.4}$), cancrinite
50 ($\text{Na}_8\text{Al}_6\text{Si}_6\text{O}_{24}(\text{CO}_3)(\text{H}_2\text{O})_2$), calcite (CaCO_3) and grossular ($\text{Ca}_3\text{Al}_2\text{Si}_3\text{O}_{12}$). These
51 highly buffered minerals have the ability to continuously dissolve and release basic
52 anions (OH^- , CO_3^{2-} and $\text{Al}(\text{OH})_4^-$) (Kong et al. 2017b). As a consequence, problems
53 such as crystalline bloom, alkaline aggregate reaction and steel corrosion will occur,
54 which restricts its recycling and results in an extremely low utilization ratio (less than
55 10%) (Santini et al. 2011; Huang et al. 2016). Therefore, regulation of its alkalinity is
56 key to its recycling potential (Klauber et al. 2011).

57 Current research has largely focused on removal of its alkalinity, including
58 gypsum transformation, seawater neutralization, carbon dioxide (CO_2) sequestration
59 and acid neutralization (Burke et al. 2013; Courtney and Kirwan 2012; Barbhuiya et al.
60 2011). Application of gypsum has been widely used for the restoration of bauxite
61 residue disposal areas (Courtney and Timpson 2005; Xue et al. 2019b). This process,
62 relies on Ca^{2+} from the gypsum to form carbonate precipitates with alkaline substances
63 in the residue, thus inhibiting the dissolution of alkaline minerals thereby reducing pH;
64 it is however a long-term restorative process. Seawater treatment is similar to that of
65 gypsum (Burke et al. 2013; Xue et al. 2019b; Babu and Reddy 2011; Renforth et al.
66 2012). Ca^{2+} and Mg^{2+} in seawater are introduced into the bauxite residue to reduce pH,
67 but the presence of Na^+ will destroy the physical and chemical structure of the bauxite

68 residue. Also, the alumina plant needs to be close to the coast, signifying a geographical
69 restriction (Clark et al. 2015; Mayes et al. 2006; Menzies et al. 2004). Acid interaction
70 can effectively remove most of the basic compounds, but dissolved calcium and
71 aluminum in solution produce considerable quantities of liquid waste contributing to
72 secondary pollution (Burke et al. 2013; Khaitan et al. 2009; Yang et al. 2016;
73 Couperthwaite et al.2013). CO₂ sequestration involves reactions between CO₂ and
74 hydroxide to form carbonate and bicarbonate, but it also promotes the dissolution of
75 chemical bonded alkali such as tri-calcium aluminate (TCA) (Sahu et al. 2010; Han et
76 al. 2017; Jones et al. 2006). In addition, CO₂ sequestration requires a high pressure
77 atmosphere to maintain sufficient interaction between reactants, which increases
78 operation cost (Smith 2009; Khaitan and Dzombak 2009).

79 Biomass transformation of bauxite residue is mainly attributed to microbial
80 fermentation processes and production of metabolites to reduce alkalinity and improve
81 its physical and chemical properties (Courtney and Harrington 2012; Jones et al 2012;
82 You et al. 2019). It is emerging as a promising in-situ remediation method for bauxite
83 residue disposal areas (Khaitan et al. 2010). Ren et al. (2017) discovered that the pH of
84 bauxite residue decreased from 10.60 to 8.96 following addition of 20% (w/w) vinegar
85 or furfural residues (Ren et al. 2017). The effect of furfural residue on pH reduction
86 was greater than with vinegar residue. Furfural residue is more acidic and contains
87 approximately 5% surface functional groups including -NH₂, -OH and other free acids,
88 which promote a faster pH drop. Courtney and Harrington (2012) demonstrated that
89 addition of mushroom compost biomass improved the residues physicochemical
90 properties and reduced its alkalinity. Although pH reduction from biomass treatments
91 is inferior when compared to other methods, it is more appealing to use accessible
92 biomass as a mild alkali modifier.

93
94
95
96
97

98 This work investigates the effect of straw and bagasse biomass on bauxite residue
99 alkalinity neutralization following biological fermentation. The effects of biomass
100 dosage and application methods on the neutralization effect of bauxite residue alkalinity
101 are also investigated. Development of pH following natural fermentation processes was
102 assessed and optimized.

104 **2 Materials and methods**

105 **2.1 Sample collection and processing**

106 Fresh bauxite residue samples were collected from Pingguo refinery (Aluminum
107 Corporation of China), in south-west China (Latitude 23°18'28.68" N, Longitude
108 107°31'8.15" E). Three subsamples were collected with a distance of 5 meters from
109 each sampling point. Samples were placed into polyethylene bags and brought back to
110 the laboratory. Samples were firstly air-dried at 65 °C for 72 h, and subsequently sieved
111 <2 mm. As local biomass recycling materials, rice straw and bagasse were selected as
112 treatments. They were allowed to air-dry naturally, pulverized and then sieved to <2
113 mm before use.

115 **2.2 Biomass investigations**

116 Bauxite residue (50 g) was weighed into plastic containers. The residues were then
117 treated as follows: straw mulching (SC), straw mixing (SM), bagasse mulching (BC)
118 and bagasse mixing (BM). Rice straw and bagasse were added to each treatment as 2,
119 4, 6, 8, 10, 20, 30 and 40% weight/weight. Hereafter BR refers to the un-treated bauxite
120 residue. Milli-Q water was then added until a solid-liquid ratio 1:5 was achieved. After
121 applying the treatments, all samples were placed on a shaker at 120 rpm (25 °C) and
122 shaken for 30 d. Each treatment was carried out in triplicate. Samples were then
123 centrifuged at 4000 r/min for 20 min and the suspensions analyzed for pH, EC and
124 soluble cations. Transformed residual solids were washed twice with Milli-Q water then
125 over-dried at 65 °C. Subsequently, the dried solids were crushed in a mortar to
126 disaggregate and sieved to retain the <2 mm fraction.

2.3 Sample characterization

pH was immediately determined in all experiments using a PHS-3C and the concentration of OH^- was calculated from pH data. CO_3^{2-} was analyzed by indicator-neutralization titration using 0.002 M H_2SO_4 (Kirwan et al. 2013). Determination of element concentrations (Al, Ca, Na, Mg and K) was carried out using Inductively Coupled Plasma Auto Emission Spectrometry (Optima 5300 DV; PerkinElmer, Waltham, MA, USA) and the $\text{Al}(\text{OH})_4^-$ was calculated from the Al concentration.

Phase compositions of dried bauxite residue samples were analysed on a Bruker D8 discover 2500 X-ray diffraction (XRD). XRD patterns were collected from 10 to 80° at a $0.04^\circ 2\theta$ step size and a $1^\circ 2\theta \text{ min}^{-1}$ scan rate. The PANalytical analysis package was used to identify and quantify phases from XRD data. The amount of amorphous material in the sample was fitted and calculated by Jade v.7 software.

Near-edge X-ray absorption fine structure (Na-XANES) and soft X-ray scanning transmission microscopy (STXM) of Na were performed on the BL08U1A beamline of the Shanghai Synchrotron Radiation Facility (SSRF). Samples were uniformly prepared on a conductor copper substrate that fixed on the sample holder through a ceramic sheet. The substrate was connected to the current amplifier through a wire. Standard spectra of sodium were collected from Na_2CO_3 and cancrinite. Sodium K-edge spectra of the photon energy in the range of 1065-1095 eV were collected by a double crystal monochromator consisting of beryllium (100 reflections). The mode of total yield detection was used with a 1 s counting time and 0.1 eV step. Athena 1.2.11 was used to normalize and average the NEXAFS spectra. The distribution of Na in samples was analyzed by STXM.

3 Results and discussion

3.1 pH

pH of the supernatants from the various treatments are displayed in Table 1. Following mulching with 2% straw, pH decreased from 10.26 to 9.97. Leachate pH decreased continuously with increasing straw volume. At 20% straw, pH decreased to 8.76. Following mulching with straw at 40%, pH decreased to 9.79. At 2% straw mixing,

158 supernatant pH was reduced to 10.08. At 20% straw mixing, pH decreased to 8.99. The
159 effect of bagasse mulching and mixing on pH transformation was similar to that of straw.
160 At 2% mulching with bagasse, leachate pH decreased to 9.96. When the dosage of
161 bagasse increased to 20%, pH decreased to 8.56. Mixing with 20% bagasse, decreased
162 pH to 8.75, indicating a lower pH decrease as compared to that of mulching with
163 bagasse. Based on the above results, both straw and bagasse will reduce residue pH, but
164 mulching was slight better than that of mixing. An optimized dosage of straw or
165 bagasse-based biomass was estimated to be 20%, which could decrease leachate pH to
166 8.56.

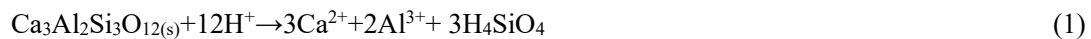
167 In the current work, it was interesting to find that the drop in pH of treated bauxite
168 residues exhibited a volcano-type trend, which presented a minimum pH with a 20%
169 biomass dosage. When the biomass ratio increased to 30% or 40%, filtrate pH showed
170 an increase as compared to that of bauxite residue treated with 20% biomass. According
171 to previous reports, (Ren et al. 2017; David et al. 2006; Patel et al. 2006) factors such
172 as fermentation temperature, substrate concentration, pH and even nitrogen source, may
173 play important roles in biomass fermentation to produce acidic species. In fact,
174 optimum acid production temperature, substrate concentration, pH and nitrogen source
175 for biomass fermentation vary greatly. For straw and bagasse fermentation in the current
176 work, the drop in pH for the 30% or 40% biomass may be attributed to the above
177 analysis. The straw or bagasse provides the carbon source for microbial growth and
178 reproduction, a low substrate concentration cannot meet the growth requirements of
179 microorganisms, whilst too high a substrate concentration would inhibit the growth of
180 microorganisms (Klinke et al. 2004; Mondala et al. 2015) Meanwhile, increased
181 biomass dosages would lead to a disruption in the balance for anaerobic and aerobic
182 fermentation in the system, which may affect acid production performance and result
183 in a decline in pH compared to bauxite residue with a lower biomass ratio.

184 **3.2 Mineralogy**

185 XRD was applied to analyze mineral phases (Fig. 1). From quantitative
186 calculations of the various phases (Table 2) with different biomass treatment, we
187 concluded that alkaline minerals from bauxite residue were significantly transformed

188 during the investigation. The primary alkaline minerals from BR were indexed to
189 andradite ($\text{Ca}_3(\text{Fe}_{0.87}\text{Al}_{0.13})_2(\text{SiO}_4)_{1.65}(\text{OH})_{5.4}$), cancrinite ($\text{Na}_8\text{Al}_6\text{Si}_6\text{O}_{24}(\text{CO}_3)(\text{H}_2\text{O})_2$),
190 calcite (CaCO_3), and grossular ($\text{Ca}_3\text{Al}_2\text{Si}_3\text{O}_{12}$) (Kong et al. 2017b). The quantified XRD
191 results (Table 3) indicate that BR contained 49.6% alkaline phases, which originated
192 from the bauxite source, digestion conditions and CaO addition (Liao et al. 2015). The
193 alkaline phase content in SC decreased from 44.8% and 45.2% in the case of BC. This
194 value decreased to 44.2% and 45.0% in SM and BM, respectively. Thus the above
195 biomass transformation investigations exhibited little effect on the change of total
196 alkaline mineral content in bauxite residues. As well, no new characteristic peaks were
197 observed from XRD patterns, suggesting there no new insoluble mineral phases were
198 formed.

199 Peaks for grossular in XRD patterns were not observed in SC, SM, BC and BM
200 although they existed in BR (Figure 1). It may be concluded that alkaline grossular
201 minerals decompose completely following fermentation of straw and bagasse (as shown
202 in Eq. (1)) (Zhang et al. 2011).



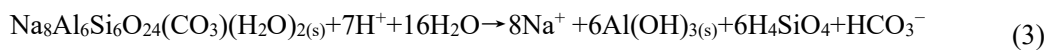
203 Peaks for andradite were observed in all bauxite residue samples (BR, SC, SM,
204 BC and BM). This means that andradite was not involved in chemical conversion
205 during the biomass fermentation process, and it was still present in bauxite residues. As
206 shown in Table 3, andradite content increased, which was caused by the dissolution of
207 other minerals in the residue and the reduction in total alkaline minerals (Grafe et al.
208 2011).

209 Characteristic peaks for calcite were observed in XRD patterns from both un-
210 transformed and biomass transformed bauxite residues. Quantitative analysis indicated
211 that the content of calcite in SC, SM, BC and BM declined following biomass mulching
212 and mixing, but this decrease was not obvious as compared with that of BR. According
213 to previous research, the neutralization reaction between calcite and acid may be
214 presented as Eq. (2), but due to the limitation in solubility, dissolved calcite was
215 relatively small (Genç-Fuhrman et al. 2004). CO_2 will be produced during the
216 dissolution process of calcite, and CO_2 is also a product during the decomposition of

217 biomass (Sharif et al. 2011). When the dissolution process of calcite and the microbial
218 respiration process are carried out simultaneously, it may have a certain inhibitory
219 effect on the dissolution reaction of calcite.



220 Cancrinite exhibited some solubility following straw and bagasse transformation
221 (Eq. (3)) (Zhu et al. 2015), but solubility varied between treatments. Following mixing
222 of straw or bagasse, cancrinite decreased by approximately 6%, but was reduced to 12%
223 with straw mulching and 15% with bagasse mulching. This may be attributed to
224 bagasse decomposition products containing more H^+ , which is favorable to the
225 dissolution of cancrinite.



226

227 3.3 Morphology characteristics

228 Na K-edge X-ray absorption near edge structure (XANES) spectra (Figure 2)
229 reveals that un-transformed bauxite residue displays two prominent absorption peaks,
230 b (located at 1076.2 eV) and e (located at 1080.0 eV). The normalized adsorption
231 intensity for peak b and peak e is 1.02 and 1.23, respectively. Two prominent absorption
232 peaks, b (1076.3 ± 0.1 eV) and peak e (1080.0 ± 0.1 eV), are also detected in the XANES
233 spectrum of transformed bauxite residues, with normalized intensities of 1.02 and 1.24.
234 Cancrinite was selected as the reference material and the prominent absorption peaks
235 are also located at 1076.2 eV and 1080.0 eV, with normalized intensities still at 1.02
236 and 1.24. Consequently, the main characteristic XANES peaks of the SC, SM, BC, BM
237 and BR are noticeably consistent with the intensity and position of the absorption peaks
238 for cancrinite. During bauxite residue transformation following addition of different
239 biomass products, cancrinite Na speciation was not significantly changed (Neuvillle et
240 al. 2004). Therefore, the decomposition process did not change the chemical form of
241 Na in bauxite residue but caused partial dissolution of cancrinite.

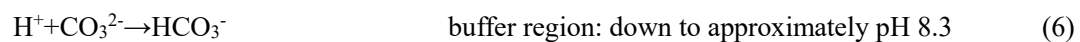
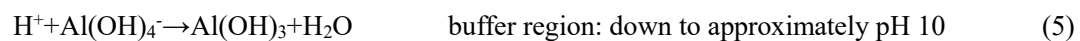
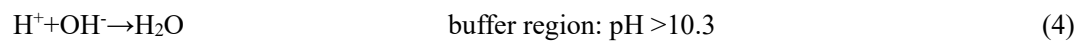
242 STXM images for Na in bauxite residue following addition of the various biomass
243 treatments is presented in Figure 3. For the BR, Na elements are strongly and densely
244 distributed in the images with spatial resolution of 30-50 nm. The spatial distribution

245 of Na with straw and bagasse is slightly weakened, but the difference is not obvious.
246 Only the mesoporous spatial distribution of Na on the fine particles becomes sparse.
247 The regulation of straw and bagasse did not change the Na speciation in bauxite residue.

248

249 **3.4 Solution chemistry**

250 The decrease in pH is directly related to the forms of alkaline anions (OH^- ,
251 $\text{Al}(\text{OH})_4^-$ and CO_3^{2-}) in the supernatant of bauxite residue (Table 3) (Gomes et al. 2016).
252 Based on previous studies, alkaline anions may be exhausted by the following reactions
253 (Eqs. (4)–(6))(Kong et al. 2017a). During biomass transformation, the concentration of
254 alkaline anions decreased significantly. Therefore, after biomass transformation, the
255 content of soluble alkali in the bauxite residue decreased, resulting in a decrease in pH.
256 The type of biomass has little difference in the transformation of alkaline anions.



257 Electrical conductivity (EC) of SC, SM, BC and BM supernatants increased
258 significantly (from 1.80 ms/cm to 3.65, 3.02, 3.45 and 2.72), mainly due to the
259 dissolution of soluble cations in bauxite residue (Table 4) (Kong et al. 2017c). The
260 content of soluble Na^+ for the supernatant transformed by the different biomass
261 products increased significantly (Table 4). With straw and bagasse mulching, Na^+
262 content doubled, but was less than that of bauxite residue treated by mixing. This may
263 be attributed to partial dissolution of soluble alkali in the bauxite residue, such as NaOH ,
264 Na_2CO_3 , NaHCO_3 and $\text{NaAl}(\text{OH})_4$. Soluble Ca^{2+} content in the supernatant
265 increased after transformation by biomass (23–40 mg/L) (Table 4). Calcium contained
266 in the bauxite residue dissolved into solution. Most of the grossular in the bauxite
267 residue dissolved into solution, which is confirmed by the disappearance of the
268 characteristic peak of grossular in the XRD pattern. Potassium and Mg^{2+} in supernatants
269 following treatments was also significantly changed (Table 4). Straw and bagasse
270 contain K^+ and Mg^{2+} , and their decomposition leads to an increase in the total amount
271 of cations in solution. Due to the different dissolved concentrations of K^+ and Mg^{2+} in
272 supernatants from straw and bagasse, it is difficult to determine the specified amount
273 of K^+ and Mg^{2+} from the bauxite residue. No soluble Fe was expected to exist in the

274 supernatant of BR, but it occurred in residues following treatment with the different
275 biomass products. Changes in supernatant soluble Fe concentrations may be due to
276 differences in straw and bagasse Fe contents.

277

278 **4 Conclusions**

279 This work presents a new technology based on biomass to regulate the alkalinity
280 of bauxite residue. When the biomass (straw and bagasse) was added at 10-20%, the
281 alkaline conversion effect was greatest, with pH being reduced from 10.26 to 8.56.
282 Furthermore, following transformation of the biomass, alkaline grossular was
283 completely dissolved, with calcite and cancrinite being dissolved to a lesser extent.
284 Straw and bagasse mulching, and straw and bagasse mixing did not change the meso-
285 scale spatial distribution of Na^+ . Determination of supernatants revealed that basic
286 anions (OH^- , CO_3^{2-} and $\text{Al}(\text{OH})_4^-$) were significantly reduced following biomass
287 decomposition. This study provides a potential application for the use of accessible
288 biomass as a green and cost effective alkali modifier for bauxite residue disposal areas.

289

290 **Acknowledgements** This work was supported by National Natural Science
291 Foundation of China (Grant No. 41877511, 41701587).

292

293 **References**

- 294 Babu AG, Reddy MS (2011) Influence of arbuscular mycorrhizal fungi on the growth
295 and nutrient status of bermudagrass grown in alkaline bauxite processing residue.
296 *Environ Pollut* 159(1):25-29
- 297 Barbhuiya SA, Basheer PAM, Clark MW, Rankinb GIB (2011) Effects of seawater-
298 neutralised bauxite refinery residue on properties of concrete. *Cement Concrete*
299 *Comp* 33(6):668-679
- 300 Burke IT, Peacock CL, Lockwood CL, Stewart DI, Mortimer RJ, Ward MB, Renforth
301 P, Gruiz K, Mayes WM (2013) Behavior of Aluminum, Arsenic, and Vanadium
302 during the Neutralization of Red Mud Leachate by HCl, Gypsum, or Seawater.
303 *Environ Sci Technol* 47(12):6527-35

304 Clark MW, Johnston M, Reichelt-Brushett AJ (2015) Comparison of several different
305 neutralisations to a bauxite refinery residue: Potential effectiveness environmental
306 ameliorants. *Appl Geochem* 56:1-10

307 Couperthwaite SJ, Johnstone DW, Millar GJ, Frost RL (2013) Neutralization of Acid
308 Sulfate Solutions Using Bauxite Refinery Residues and Its Derivatives. *Ind Eng*
309 *Chem Res* 52(4):1388–1395

310 Courtney R, Harrington T (2012) Growth and nutrition of *Hocus lanatus* in bauxite
311 residue amended with combinations of spent mushroom compost and gypsum.
312 *Land Degrad Dev* 23(2):144-149

313 Courtney R, Kirwan L (2012) Gypsum amendment of alkaline bauxite residue – Plant
314 available aluminium and implications for grassland restoration. *Ecol Eng* 42:279-
315 282

316 Courtney RG, Timpson JP (2005) Reclamation of Fine Fraction Bauxite Processing
317 Residue (Red Mud) Amended with Coarse Fraction Residue and Gypsum. *Water*
318 *Air Soil Poll* 164(1–4):91-102

319 David RD, Richard A G (2007) Chemicals from Biomass. *Science* 318:1249-1250

320 Genç-Fuhrman H, Tjell JC, McConchie D (2004) Increasing the arsenate adsorption
321 capacity of neutralized red mud (Bauxsol). *J Colloid Interf Sci* 271(2):313–320.

322 Gomes HI, Mayes WM, Rogerson M, Stewart DI, Burke IT (2016) Alkaline residues
323 and the environment: a review of impacts, management practices and opportunities.
324 *J Clean Prod* 112(4):3571-3582

325 Grafe M, Power G, Klauber C (2011) Bauxite residue issues: III. Alkalinity and
326 associated chemistry. *Hydrometallurgy* 108(1-2):60-79

327 Han YS, Ji S, Lee PK, OH C (2017) Bauxite residue neutralization with simultaneous
328 mineral carbonation using atmospheric CO₂. *J Hazard Mater* 326:87-93

329 Huang L, Li YW, Xue SG, Zhu F, Wu C, Wang QL (2016) Salt composition changes
330 in different stacking ages of bauxite residue. *T Nonferr Metal Soc* 26: 2433-2439
331 (In Chinese)

332 Jones BEH, Haynes RJ, Phillips IR (2012) Addition of an organic amendment and/or
333 residue mud to bauxite residue sand in order to improve its properties as a growth
334 medium. *J Environ Manage* 95(1):29-38

335 Jones G, Joshi G, Clark MW, McConchie DM (2006) Carbon Capture and the
336 Aluminium Industry: Preliminary Studies. *Environ Chem* 3(4)

337 Klinke HB, Thomsen AB, Ahring BK (2004) Inhibition of ethanol-producing yeast and
338 bacteria by degradation products produced during pre-treatment of biomass. *Appl*
339 *Microbiol Biotechnol* 66: 10–26

340 Khaitan S, Dzombak DA, Lowry GV (2009) Chemistry of the Acid Neutralization
341 Capacity of Bauxite Residue. *Environ Eng Sci* 26(5):873-881

342 Khaitan S, Dzombak DA, Lowry GV (2009) Mechanisms of Neutralization of Bauxite
343 Residue by Carbon Dioxide. *J Environ Eng* 135(6):433-438

344 Khaitan S, Dzombak DA, Swallow P, Schmidt P, Fu J, Lowry GV (2010) Field
345 Evaluation of Bauxite Residue Neutralization by Carbon Dioxide, Vegetation, and
346 Organic Amendments. *J Environ Eng* 136(10):1045-1053

347 Kirwan LJ, Hartshorn A, Mcmonagle JB, Fleming L, Funnell D (2013) Chemistry of
348 bauxite residue neutralisation and aspects to implementation. *Int J Miner Process*
349 119:40-50

350 Klauber C, Gräfe M, Power G (2011) Bauxite residue issues: II. options for residue
351 utilization. *Hydrometallurgy* 108(1-2):11-32

352 Kong XF , Guo Y , Xue SG, Hartley W, Wu C, Ye YZ, Cheng QY (2017c) Natural
353 evolution of alkaline characteristics in bauxite residue. *J Clean Prod* 143:224-230

354 Kong XF, Jiang XX, Xue SG, Huang L, Hartley W, Wu C, Li XF (2018) Migration and
355 distribution of saline ions in bauxite residue during water leaching. *T Nonferr*
356 *Metal Soc* 28(3):534-541

357 Kong XF, Li M, Xue SG, Hartley W, Chen CR, Wu C, Li XF, Li YW (2017a) Acid
358 transformation of bauxite residue: conversion of its alkaline characteristics. *J*
359 *Hazard Mater* 324:382-390

360 Kong XF, Tian T, Xue SG, Hartley W, Huang LB, Wu C, Li CX (2017b) Development
361 of alkaline electrochemical characteristics demonstrates soil formation in bauxite
362 residue undergoing natural rehabilitation. *Land Degrad Dev* 29(1):58-67

363 Li XF, Ye YZ, Xue SG, Jiang J, Wu C, Kong XF, Hartley W, Li YW (2018) Leaching
364 optimization and dissolution behavior of alkaline anions in bauxite residue. *T*
365 *Nonferr Metal Soc* 28(6):1248-1255

366 Liao CZ, Zeng L, Shih K (2015) Quantitative X-ray Diffraction (QXRD) analysis for
367 revealing thermal transformations of red mud. *Chemosphere* 131:171-177

368 Mayes W M, Younger P L, Jonathan A (2006) Buffering of Alkaline Steel Slag
369 Leachate across a Natural Wetland. *Environ Sci Technol* 40(4):1237-1243

370 Menzies NW, Fulton IM, Morrell WJ (2004) Seawater Neutralization of Alkaline
371 Bauxite Residue and Implications for Revegetation. *J Environ Qual* 33(5):1877-84

372 Mondala AH (2015) Direct fungal fermentation of lignocellulosic biomass into itaconic,
373 fumaric, and malic acids: current and future prospects. *J Ind Microbiol Biotechnol*
374 42:487–506

375 Neuville DR, Cormier L, Flank AM, Prado RJ, Lagarde P (2004) Na K-edge XANES
376 spectra of minerals and glasses. *Eur J Mineral* 16:809-816

377 Patel MA, Ou MS, Harbrucker R, Aldrich HC, Buszko ML, Ingram LO, Shanmugam
378 KT (2006) Isolation and Characterization of Acid-Tolerant, Thermophilic Bacteria
379 for Effective Fermentation of Biomass-Derived Sugars to Lactic Acid. *Appl*
380 *Environ Microb* 72: 3228–3235

381 Power G, Gräfe M, Klauber C (2011) Bauxite residue issues: I. Current management,
382 disposal and storage practices. *Hydrometallurgy* 108(1-2):33-45

383 Ren J, Liu JD, Chen J, Liu XL, Li FS, Du P (2017) Effect of ferrous sulfate and
384 nitrohumic acid neutralization on the leaching of metals from a combined bauxite
385 residue. *Environ Sci Pollut R* 24(10): 9325–9336

386 Renforth P, Mayes WM, Jarvis AP, Burke IT, Manning DAC, Gruiz K (2012)
387 Contaminant mobility and carbon sequestration downstream of the Ajka (Hungary)
388 red mud spill: The effects of gypsum dosing. *Sci Total Environ* 421-422:253-259

389 Sahu RC, Patel RK, Ray BC (2010) Neutralization of red mud using CO₂ sequestration
390 cycle. *J Hazard Mater* 179(1-3):28-34

391 Santini TC, Fey MV (2015) Fly ash as a permeable cap for tailings management:
392 pedogenesis in bauxite residue tailings. *J Soil Sediment* 15(3):552-564

393 Santini TC, Fey MV (2018) From tailings to soil: long-term effects of amendments on
394 progress and trajectory of soil formation and in situ remediation in bauxite residue.
395 *J Soil Sediment* 18(5):1935-1949

396 Santini TC, Hinz C, Rate AW, Carterb CM, Gilkesa RJ (2011) In situ neutralisation of

397 uncarbonated bauxite residue mud by cross layer leaching with carbonated bauxite
398 residue mud. *J Hazard Mater* 194:119-127

399 Sharif MSU, Davis RK, Steele KF, Kim B, Hays PD, Kresse TM, Fazio JA (2011)
400 Surface complexation modeling for predicting solid phase arsenic concentrations
401 in the sediments of the Mississippi River Valley alluvial aquifer, Arkansas, USA.
402 *Appl Geochem* 26(4):496–504.

403 Smith P (2009) The processing of high silica bauxites — Review of existing and
404 potential processes. *Hydrometallurgy* 98(1-2):162-176

405 Xu BA, Smith P, Wingate C, Silva LD (2010) The effect of calcium and temperature
406 on the transformation of sodalite to cancrinite in Bayer digestion. *Hydrometallurgy*
407 105(1-2):75-81

408 Xue SG, Kong XF, Zhu F, Hartley W, Li XF, Li YW (2016a) Proposal for management
409 and alkalinity transformation of bauxite residue in China. *Environ Sci Pollut R*
410 23(13):12822-12834

411 Xue SG, Li M, Jiang J, Millar GJ, Li CX, Kong XF (2019b) Phosphogypsum
412 stabilization of bauxite residue: Conversion of its alkaline characteristics. *J*
413 *Environ Sci-China* 77:1-10

414 Xue SG, Wu YJ, LI YW, Kong XF, Zhu F, Hartley W, Li XF, Ye YZ (2019a) Industrial
415 wastes applications for alkalinity regulation in bauxite residue: a comprehensive
416 review. *J Cent South Univ* 26(2):268-288

417 Xue SG, Zhu F, Kong XF, Wu C, Huang L, Huang N, Hartley W (2016b) A review of
418 the characterization and revegetation of bauxite residues (Red mud). *Environ Sci*
419 *Pollut R* 23(2): 1120–1132

420 Yang Y, Wang XW, Wang MY, Wang HG, Xian PF (2016) Iron recovery from the
421 leached solution of red mud through the application of oxalic acid. *Int J Miner*
422 *Process* 157(10):145-151

423 You F, Zhang LP, Ye J, Huang LB (2019) Microbial decomposition of biomass residues
424 mitigated hydrogeochemical dynamics in strongly alkaline bauxite residues. *Sci*
425 *Total Environ* 663:216-226

426 Zhang R, Zheng SL, Ma SH, Zhang Y (2011) Recovery of alumina and alkali in Bayer
427 red mud by the formation of andradite-grossular hydrogarnet in hydrothermal

428 process. J Hazard Mater 189(3):827-835

429 Zhu F, Hou JT, Xue SG, Wu C, Wang QL, Hartley W (2017) Vermicompost and
430 Gypsum Amendments Improve Aggregate Formation in Bauxite Residue. Land
431 Degrad Dev 28(7): 2109-2120

432 Zhu F, Zhou JY, Xue SG, Hartley W, Wu C, Guo Y (2016) Aging of bauxite residue in
433 association of regeneration: a comparison of methods to determine aggregate
434 stability & erosion resistance. Ecol Eng 92(3):47-54

435 Zhu XB, Li W, Guan XM (2015) An active dealcalization of red mud with roasting and
436 water leaching. J Hazard Mater 286:85–91
437